35th Annual International Conference of the IEEE EMBS
Osaka, Japan, 3 - 7 July, 2013

Detection of cigarette smoke inhalations from respiratory signals using reduced feature set

Yogendra Patil, Paulo Lopez-Meyer, Stephen Tiffany and Edward Sazonov, *Senior Member, IEEE*

Abstract— **A combination of wearable Respiratory Inductive Plethysmograph and a hand-to-mouth Proximity Sensor (PS) can be used to monitor smoking habits and smoke exposure in cigarette smokers. In our previous work, detection of smoke inhalations was achieved by using a Support Vector Machine (SVM) classifier applied to raw sensor signals with 1503-element feature vectors. This study uses empirically-defined 27 features computed from the sensor signals to reduce the length of vectors. Further reduction in the length of the feature vectors was achieved by a forward feature selection algorithm, identifying from 2 to 16 features most critical for smoke inhalations detection. For individual detection models, the 1503-element feature vectors, 27-element feature vectors and reduced feature vectors resulted in F-scores of 90.1%, 68.7% and 94% respectively. For the group models, F-scores were 81.3%, 65% and 67% respectively. These results demonstrate feasibility of detecting smoke inhalations with a computed feature set, but suggest high individuality of breathing patterns associated with smoking.**

I. Introduction

Cigarette Smoking is the cause of cancer, heart disease, stroke, and lung diseases (including emphysema, bronchitis, and chronic airway obstruction) [1]. About 90 percent of lung cancer deaths and about 80-90 percent of COPD (emphysema and chronic bronchitis) deaths are caused by cigarette smoking [2]. It is of clinical importance to develop an efficient methodology in order to understand the behaviors associated with this habit. Such a methodology should be able to accurately identify the number of cigarettes smoked in a given time duration, the volume of smoke inhaled, the duration of smoke holding, etc. in order to improve the effectiveness of pharmacological interventions. The simplest and most common method to assess smoking behavior is by asking subjects to report how many cigarettes they consume. But a self-report can provide only a crude estimate of cigarette consumption, as the accuracy of the report is limited by memory bias and intentional under reporting [3]. Other methods rely on portable smoking topography devices, which allow the evaluation of smoking frequency and puffing behavior in free-living conditions [4]. Although these devices overcome some of the problems associated with a self-report, they require users to smoke through the device. Failing to do so causes loss of the puff topography data [4]. Machine Vision techniques have also been used to detect smoking events [5]. Although the results have shown effectiveness of the technique in smoking event analysis, these methods are limited to a specific location equipped with video cameras.

The PACT (Personal Automatic Cigarette Tracker) system was developed to achieve reliable monitoring of cigarette smoking behavior in free-living conditions, without interfering with the natural smoking behavior of the individual [6], [7]. PACT combines a wearable Respiratory Inductive Plethysmograph (RIP) and a hand-to-mouth Proximity Sensor (PS) to monitor and recognize characteristics hand gestures and breathing patterns specific to smoke inhalations. When fully developed, PACT will be used as a research tool for studying cigarette smoking and for measuring effectiveness of smoke cessation interventions.

In our previous work, a SVM classifier was developed to detect smoke inhalations using raw sensor signals from PACT forming 1503-element feature vectors [6]. The main goals of this work are: a) use computed features rather that raw sensor signals to reduce the dimensionality of feature vectors, b) select the best feature set by applying a forward feature selection algorithm.

II. Methodology

A. Sensor System

A non-invasive wearable sensor system was developed to capture these breathing and hand-to-mouth gesture patterns [6], [7]. Breathing was monitored by a wearable Respiratory Inductance Plethysmograph (RIP, Pro-Tech Inc., Fig. 1 (c)) module consisting of thoracic (Fig.1 (a)) and abdominal (Fig.1 (b)) elastic respiratory bands (DuraBelt, Pro-Tech Inc.). The RIP system captured the change in breath volume, proportional to the subject's lungs expansion and contraction [8]. The hand-to-mouth gestures were detected using a radio frequency (RF) operated proximity sensor consisting of a transmitter positioned on the wrist of the subject's dominant hand (Fig. 1 (d)) and a receiver positioned on the chest (Fig. 1 (e)) [7]. The RIP output signals were, $TC(t)$ and $AB(t)$ from the thoracic and abdominal bands, respectively, and the PS output signal, $PS(t)$, were recorded at a sample rate of 100 Hz by a portable data logger (Logomatic V2.0, Sparkfun Inc.) (Fig. 1 (f)). A micro-SD card with a storage capacity of 2Gb was used to store data. The stored data was further used to perform off-line analysis.

B. Data Collection

Data was collected from 20 regular smokers (Table I). All subjects reported to be healthy with no chronic respiratory problems and no allergies. The study protocol was approved by the University of Alabama IRB. Each subject performed 12 different activities specifically selected so that they represent everyday activities, varying in both hand gestures and breathings patterns (Table II). Each experiment was videotaped so as to perform manual annotation of the activities, with the annotations being used as the gold standard for development of the classification techniques.

C. Signal Pre-Processing

All signals were synchronized to a common time scale. The proximity signal $PS(t)$ was normalized to a scale of 0 to 1. The tidal volume signal ($VT(t)$) was calculated as the average between the $TC(t)$ and the $AB(t)$ signals obtained from the RIP sensors: $VT(t) = (TC(t)+AB(t))/2$ (1)

The $VT(t)$ signal was then scaled in amplitude to a range of -1.0 to 1.0 using the min-max normalization. An ideal band pass filter, with cut-off frequencies between 0.0001 and 10 Hertz, was applied to reduce artifacts and eliminate baseline drift of the respiration signal. The signal was denoised by a moving average algorithm.

The airflow signal $AS(t)$ was calculated from the filtered and denoised $VT(t)$ signal. An airflow signal $AS(t)$ is defined as the rate of change of tidal volume signal over time and was computed as [8]: $AS(t) = dVT(t)/dt$, (2)

Pre-processed $PS(t)$, $VT(t)$ and $AS(t)$ signals were used for feature extraction as described in the following section.

Figure 1. The PACT system, (a) Thoracic elastic band, (b) Abdominal elastic band, (c) electronic module for the portable Plethysmograph (RIP), (d) wrist worn RF transmitter of the PS system, (e) chest mounted RF receiver of the PS system, (f) data logger.

TABLE I. DEMOGRAPHIC INFORMATION FOR 20 SUBJECTS

Number of Subjects	20 (10 males, 10 females)
Age	23.1 $\pm$ 3.3 years
BMI	25.88 $\pm$ 5.24 kg/m^2
Smoking history	> 1year
CO for breath sample	> 10 ppm

TABLE II. ACTIVITIES PERFORMED AND THEIR DURATION

Activity	Name of the Activity	Time Length (min)
1	Sit silently	5
2	Read loudly	5
3	Stand still	5
4	Walk on treadmill at self-selected slow pace	5
5	Walk on treadmill at self-selected fast pace	5
6	Browse internet on laptop	5
7	Eat food without using silverware and drink directly from cup	Unrestricted time
8	Eat food using silverware and drink using a straw	Unrestricted time
9	Walk outside the building	5
10	Smoke a cigarette in sitting position	Unrestricted time
11	Rest in sitting position	5
12	Smoke a cigarette in standing position	Unrestricted time

D. Feature Extraction

A total of 27 features were extracted from the $VT(t)$, $AS(t)$ and $PS(t)$ signals (Fig. 2). The features were only extracted for breathing cycles where a hand-to-mouth gesture, detected from the PS, was present. The increase in amplitude of the PS signal represents an event of a hand-to-mouth gesture, which could be related to eating, smoking, etc. Features extracted from the $PS(t)$ characterized a typical hand-to-mouth gesture from the smoking activity and that from $AS(t)$ and $VT(t)$, characterized the typical respiratory activity during a smoke inhalation. A smoke inhalation typically starts with an apnea period (cessation of normal air-intake due to a puff, or smoke inhalation into the mouth) concurrent with a hand-to-mouth gesture. At the end of the hand-to-mouth gesture a sudden drop in the amplitude of the PS signal (as the cigarette is removed from the mouth) and a sharp increase in tidal volume and airflow, which represents the cigarette smoke inhalation into the lungs, are observed. The deep inhalation is then followed by a period of smoke holding and an exhale. Using this *a-priori* knowledge of typical behavior for smoking, the features computed for $PS(t)$, $AS(t)$ and $VT(t)$ are listed in Table III.

For each one of the hand-to-mouth gestures detected $\{HMG_i\}$, i = 1,2,…,n, a feature vector f_i was constructed from PS(t), VT(t) and AS(t). All features were normalized within a range of -1 to +1. The described features can be defined as: $f_i = \{PS_i^4, VT_i^{10}, AS_i^{13}\}$. (3)

Labels were assigned to each feature f_i as $L_i = \{-1, 1\}$; $L = -1$ if the feature vector was not associated with a smoke inhalation and $L = 1$ if the feature vector was associated with a smoke inhalation. The dataset pairs $F_i^{\,j}\{f_i^j, L_i^j\}$, for $j = 1,2,\ldots,20$ subjects, were used to train a SVM classifier.

E. Support Vector Machine Classifier

The SVM classifier was chosen as it has shown a reliable performance over a variety of different data sets [9] [10]. In this study the SVM classifier was used to predict whether a given set of features was related to smoke inhalations or non-smoking breaths. The implementation of SVM models was performed using the LibSVM package [11]. The accuracy of SVM classification depends on the selection of kernel, the kernel's parameters and the soft margin parameter C. The radial basis kernel function was selected for the SVM models, since they can generate a nonlinear decision boundary [10]. Each combination for parameter choice, cost value C and kernel's gamma value γ, was checked using cross-validation and the parameters with best cross-validation accuracy were picked. A simple exhaustive grid search procedure with $C = e^c$ for c = {-5… 5}, and $\gamma = e^h$ for h = {-5… 5} was used to find optimal parameters.

Two types of classification models, namely individual models and the group model were built. The Individual models are subject-dependent, and trained for a particular subject only. The global model is a subject-independent model that can be applied to any subject without the need for individual calibration. Training of Individual models was performed by applying the dataset pair F from randomly selected 5 non-smoking activities and 1 smoking activity and validation from the remaining dataset.

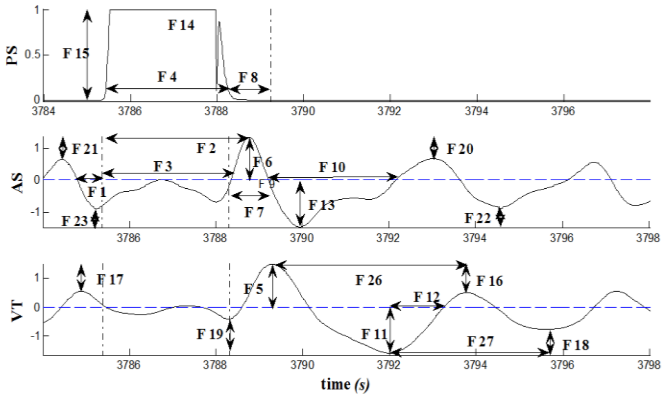

Figure 2. Features extracted from PS, AS and VT during a hand-to-mouth gesture related to smoking activity.

TABLE III. FEATURES EXTRACTED FOR PS, AS, VT

Feature #	Description
1	duration of expiration
2	time-duration from the start time of a hand gesture to peak of $AS(t)$
3	time-duration of hand-to-mouth gesture to point of air-flow exceeding a threshold [12]
4	the time duration of hand remaining at the mouth
5	peak inspiration following the hand-to-mouth gesture
6	peak inspiration following the hand-to-mouth gesture
7	inspiration duration
8	time duration of the hand removal from the mouth up to beginning of the expiration
9	duration of the smoke holding (not shown in Figure 2 due to very small duration)
10	expiration duration
11	breath volume
12	expiration duration
13	maximum expiration level
14	the mean amplitude
15	the max amplitude
16	relative difference between peak inspiration following a hand-to-mouth gesture and next peak
17	relative difference between the peak inspiration following the hand-to-mouth gesture and previous peak
18	relative difference between maximum expiration level following the hand-to-mouth gesture and the next breathing cycle's maximum expiration level
19	relative difference between maximum expiration level following the hand-to-mouth gesture and previous breathing cycle's maximum expiration level
20	relative difference between peak inspiration following hand-to-mouth gesture and subsequent peak
21	relative difference between the peak inspiration following the hand-to-mouth gesture and previous peak
22	relative difference between maximum expiration level following the hand-to-mouth gesture and next breathing cycle's maximum expiration level
23	relative difference between maximum expiration level following the hand-to-mouth gesture and previous breathing cycle's maximum expiration level
24	L2-norm of the breathing cycle related to smoking and the next breathing cycle (not shown in Figure 2)
25	L2-norm of the breathing cycle related to smoking and the next breathing cycle (not shown in Figure 2)
26	time-duration between peak inspiration following hand-to-mouth gesture and next peak
27	time-duration for occurrence of maximum expiration level following hand-to-mouth gesture and next maximum expiration level

For each subject, 2 replicates for the randomly generated training and validation set were produced and the average accuracy was computed. This procedure was implemented to avoid over-fitting of the model to the training dataset. For the group model training, a leave-one-out validation procedure was used to train and validate the classification model. From the dataset of 20 subjects, 19 were selected for training and the remaining subject was used for validation. This procedure was implemented for 20 replicates, one for each subject.

Precision (P) and Recall (R) were used as a metrics to evaluate the accuracy defined as [13]:

$$P = TP/(TP+FP) \tag{4}$$

$$R = TP/(TP+FN) \tag{5}$$

Table IV defines the three metrics TP, FP and FN using an instance for feature f_i , based on its true label L_i and SVM model predicted label L_i*, during the validation phase of the SVM model. During the training process, the F-score was used to select the optimal C and γ values for the SVM model, defined as [13]: F-score = $2\cdot (P\cdot R/(P+R))$ (6)

TABLE IV. METRICS TP, FP AND FN

METRIC	SVM MODEL PREDICTED LABEL	TRUE LABEL
TP	$f_i \in L_i^* = +1$	$f_i \in L_i = +1$
FP	$f_i \in L_i^* = +1$	$f_i \in L_i = -1$
FN	$f_i \in L_i^* = -1$	$f_i \in L_i = +1$

F. Sequential Forward Selection

. Sequential Feature Selection (SFS) procedure was employed to obtain a subset of most significant features. Implementation of SFS requires a feature set, a classifier and a selection criterion. The SFS iteratively selects features based on a certain criterion (here F-score) until the stopping condition is reached[14]. For example, in the first iteration, the SVM is trained with each individual feature (from the 27 feature vector). The feature resulting in the highest F-score is selected. In the second iteration, the SVM is trained with the combination of the selected feature and every individual feature (from remaining 26 features). The feature set resulting in the highest F-score is selected. The process continues until the F-score ceases to increase. The final subset contains the most influential features for efficient classification.

RESULTS

The results for reduced features are summarized in Table V, VI and VII. The summarized classification results for both individual and group models are grand mean of all the metrics obtained across 20 subjects.

TABLE V. CLASSIFICATION ACCURACY FOR INDIVIDUAL MODELS USING 1503, 27 AND REDUCED FEATURE SET

	F-score %	Precision %	Recall %
1503 Features	90.19±9.21	91.95±8.43	89.53±9.72
27 Features	68.67±27.28	73.48±24.28	68.38±28.85
Reduced Features	94.00±10.66	99.55±1.11	90.80±15.35

TABLE VI. FREQUENCY OF SELECTION FOR EACH FEATURE AMONG 20 SUBJECTS AFTER APPLYING SFS

Feature	# of Times Selected	Feature	# of Times Selected	Feature	# of Times Selected
F1	2	F10	2	F19	0
F2	3	F11	1	F20	0
F3	5	F12	0	F21	0
F4	9	F13	4	F22	6
F5	4	F14	11	F23	5
F6	2	F15	1	F24	2
F7	3	F16	2	F25	1
F8	3	F17	0	F26	1
F9	2	F18	1	F27	0

TABLE VII. CLASSIFICATION ACCURACY FOR THE GROUP MODEL USING 1503, 27 AND REDUCED FEATURE SET

	F-score %	Precision %	Recall %
1503 Features	81.25±16.29	87.07±13.3	80.90±21.32
27 Features	65.09±21.64	76.56±17.96	61.32±26.51
Reduced Features (16)	67.12±22.89	81.53±14.80	63.38±27.15

III. DISCUSSION AND CONCLUSIONS

This study presents a methodology for detection of smoke inhalations using features computed from respiration and proximity sensor signals. Overall, results suggest that detection of smoking from the respiratory signals collected by a wearable monitoring system is feasible with a reduced feature set.

In case of individual models, the 27 features resulted in average F-score of 68.7% and for the group model in F-score of 65%. These results are low as compared to the 1503-element feature vectors (90% and 81.3% respectively). A potential reason is that some of the 27 features, were insignificant and resulted in reduction of the classifier accuracy. The SFS algorithm was applied for the 27 features so as to select relevant features and achieve higher accuracy rate. From Table VI, feature F14 (that is, mean value of proximity sensor signal for given hand-to-mouth gesture) is selected most (11 times), as it represents the most common act (that is bringing hand towards mouth) in any cigarette smoker. Feature F4 (selected 9 times) is the second most selected feature as it represents a typical time related hand-to-mouth gesture for a smoker (that is taking hand close to mouth, take a deep inhale followed by taking hand away from mouth). The third most selected features F3, F5, F13, F22 and F23 represents the relative difference between a smoking and normal breathing activity. For example, feature F22 is the difference between smoking related maximum expiration level (which is the deep exhalation of smoke) to the following maximum expiration level (which represents the expiration of normal breathing). This difference is very particular in smoking activity, for all smokers, as compared to other activities in our study. Finally selected features such as F1, F2, F6, F7, F8, F9 and F10 are typically observed in a smoking activity. For example, feature F6 (maximum inspiration level) is commonly observed in smoking activity when the smoke is inhaled by smoker. After the application of SFS algorithm, F-score of 94% was achieved for individual models (with individual features sets of 2 to 16 features). This result is comparable to the 1503-element features. The, SFS algorithm selected the best feature set for each subject that allowed for better classification. However, the feature selection may have also resulted in overfitting of the models to features most pronounced in individual smokers. For the group model, SFS selected a total of 16 features (F2, F6, F7, F8, F9, F10, F11, F14, F15, F16, F18, F24), which resulted in F-score of 67%, or much lower than results for 1503 feature set. One potential reason is that reduced features were able to explain the variability occurred within a subject but failed to do so for variability between subjects.

In conclusion, these results demonstrate feasibility of cigarette smoking monitoring from the featured computed from the proximity and breathing sensor signals but at the same raise questions about what features best describe the smoking activity.

REFERENCES

[1] Centers for Disease Control and Prevention, "Sustaining State Programs for Tobacco control Data Highlights," 2006. [Online]. Available: http://www.cdc.gov/tobacco/data_statistics/state_data/data_highlights/2006/pdfs/dataHighlights06rev.pdf.

[2] "American Lung Association," *American Lung Association*. [Online]. Available: http://www.lung.org/stop-smoking/about-smoking/facts-figures/general-smoking-facts.html. [Accessed: 17-Jan-2013].

[3] S. S. Michael R. Hufford, "Ecological Momentary Assessment: Real-world, real-time measurement of patient experience.," 2012.

[4] D. Hammond, G. T. Fong, K. M. Cummings, and A. Hyland, "Smoking Topography, Brand Switching, and Nicotine Delivery: Results from an In vivo Study," *Cancer Epidemiol Biomarkers Prev*, vol. 14, no. 6, pp. 1370–1375, Jun. 2005.

[5] Pin Wu, Jun-Wei Hsieh, Jiun-Cheng Cheng, Shyi-Chyi Cheng, and Shau-Yin Tseng, "Human Smoking Event Detection Using Visual Interaction Clues," in *2010 20th International Conference on Pattern Recognition (ICPR)*, 2010, pp. 4344–4347.

[6] P. Lopez-Meyer, S. Tiffany, and E. Sazonov, "Identification of cigarette smoke inhalations from wearable sensor data using a Support Vector Machine classifier," in *2012 Annual International Conference of the IEEE Engineering in Medicine and Biology Society (EMBC)*, 2012, pp. 4050 – 4053.

[7] E. Sazonov, K. Metcalfe, P. Lopez-Meyer, and S. Tiffany, "RF hand gesture sensor for monitoring of cigarette smoking," in *2011 Fifth International Conference on Sensing Technology (ICST)*, 2011, pp. 426 – 430.

[8] A. Eberhard, P. Calabrese, P. Baconnier, and G. Benchetrit, "Comparison Between the Respiratory Inductance Plethysmography Signal Derivative and the Airflow Signal," in *Frontiers in Modeling and Control of Breathing*, vol. 499, C.-S. Poon and H. Kazemi, Eds. Boston, MA: Springer US, 2001, pp. 489–494.

[9] D. Meyer, F. Leisch, and K. Hornik, "The support vector machine under test," *Neurocomputing*, vol. 55, no. 1–2, pp. 169–186, Sep. 2003.

[10] P. Lopez-Meyer, S. Schuckers, O. Makeyev, and E. Sazonov, "Detection of periods of food intake using Support Vector Machines," *Conf Proc IEEE Eng Med Biol Soc*, vol. 2010, pp. 1004–1007, 2010.

[11] C.-C. Chang and C.-J. Lin, "LIBSVM: A library for support vector machines," *ACM Trans. Intell. Syst. Technol.*, vol. 2, no. 3, pp. 27:1–27:27, May 2011.

[12] A. Moreau-Gaudry, A. Sabil, G. Benchetrit, and A. Franco, "Use of respiratory inductance plethysmography for the detection of swallowing in the elderly," *Dysphagia*, vol. 20, no. 4, pp. 297–302, 2005.

[13] D. L. Olson and D. Delen, *Advanced data mining techniques*. Springer, 2008.

[14] A. Marcano-Cedeño, J. Quintanilla-Domínguez, M. G. Cortina-Januchs, and D. Andina, "Feature selection using Sequential Forward Selection and classification applying Artificial Metaplasticity Neural Network," in *IECON 2010 - 36th Annual Conference on IEEE Industrial Electronics Society*, 2010, pp. 2845 –2850.